3rd URSI AT-AP-RASC, Gran Canaria, 29 May – 3 June 2022

Quasi-Trapped Electron Fluxes Induced by NWC Transmitter and CRAND: Observations and Simulations

Zheng Xiang* (1), Binbin Ni(1), Yangxizi Liu(1) and Xinlin Li(2)
(1) Department of Space Physics, School of Electronic Information, Wuhan University, Wuhan, China
(2) Laboratory for Atmospheric and Space Physics, University of Colorado Boulder, Boulder, USA

Abstract

NWC transmitter signals can leak into the magnetosphere and scatter trapped energetic electrons into drift loss cones observed by low-Earth orbit satellites. Recent studies also suggest that cosmic ray albedo neutron decay (CRAND) is probably an important source for quasi-trapped electrons in the inner belt. To investigate the relative contributions of NWC transmitter signals and CRAND to quasi-trapped electrons, the long-term variations of quasi-trapped 206 keV electrons at L=1.7 measured by DEMETER satellite are analyzed in details. Furthermore, a drift-diffusion-source model well reproduces the longitudinal distribution of quasi-trapped electrons. These results suggest that CRAND is the main source of quasi-trapped hundreds of keV electrons when NWC station is at dayside. In contrast, pitch angle diffusions become the main source mechanism of these quasi-trapped electrons when NWC station operates at nightside with more VLF transmitter energy leaking into the magnetosphere.

1. Introduction

Due to the off-center nature of Earth's magnetic field, energetic electrons in the radiation belts can be classified into three categories: trapped, quasi-trapped, and untrapped (e.g., [1], [2]). The quasi-trapped electrons have equatorial pitch angles larger than the local bounce loss cone (BLC) but smaller than the largest BLC across their full drift orbit (the so-called drift loss cone (DLC)). Quasi-trapped electrons can compete many bounce periods before precipitating into the South Atlantic Anomaly (SAA) region where the magnetic field strength is the weakest and altitudes of quasi-trapped electrons' mirror points generally decrease to below 100 km (usually considered as the inner boundary of the inner radiation belt). Thus, the lifetime of quasi-trapped electrons is shorter than the electron drift period ranging from several minutes to a few hours in radiation belts depending on electron energies and spatial locations.

Pitch angle diffusions induced by wave-particle interactions are loss mechanisms for trapped electrons but can be sources of quasi-trapped electrons. Trapped energetic electrons can be scattered into the DLC and become quasi-trapped induced by various magnetospheric wave modes including chorus waves, plasmaspheric hiss waves, EMIC waves, and man-made VLF transmitter signals (e.g., [3], [4]). Generally, pitch angle diffusions dominate the source of quasi-trapped electrons in the radiation belts while CRAND can contributes to the quasi-trapped electrons close to the inner edge of inner belt. CRAND describes the process that albedo neutrons, which are produced by interactions between cosmic rays and atmosphere neutral species, decay into electrons, protons, and antineutrinos with a mean lifetime around 15 minutes. Using the Colorado Student Space Weather Experiment CubeSat (CSSWE), Li et al. (5) found that all energetic electrons (~ 0.5 MeV) at L <1.14 are CRAND produced. By adding a CRAND source term in previous drift-diffusion models (e.g., [6]), Xiang et al. (2) confirmed the conclusions in Li et al. (5) and further suggested that CRAND is an important source of trapped electrons at L<1.3 during quite times.

At L=1.5-2, many satellite observations have demonstrated that VLF transmitter signals, which are used for submarine communications, from NWC station at west Australia can cause significant enhancements of quasi-trapped energetic electrons with obvious day-night dependences (e.g., [7]). The wave power of VLF transmitter leaked into the magnetosphere is significantly influenced by the ionospheric profile. During night, electron densities in ionosphere become weaker, allowing stronger VLF transmitter signals after trans-ionospheric propagations. When NWC is at dayside, the flux level of quasi-trapped electron is relatively low due to weaker wave-particle interactions. As a small but constant source, CRAND may play a role in the sources of these quasi-trapped electrons. To investigate the relative contributions of CRAND and pitch angle diffusions induced by NWC transmitter signals to energetic electrons in the inner radiation belt, we investigate the long-term variations of quasi-trapped electrons measured by DEMETER satellite and simulate the longitudinal distribution of energetic electrons based on a drift-diffusion-source model including azimuthal drift, pitch angle diffusion due to NWC transmitter signals, and a CRAND source.

2. Data and Model Description

DEMETER satellite was launched into a circular Sun-synchronous orbit with ~710 km altitude in June 2004 for earthquake research at local times around 10:30 LT and

22:30 LT. The Instrument for Detection of Particle (IDP) onboard DEMETER provides electron flux measurements at 128 energy channels ranging from 70 keV to 2.5 MeV in every 4s.

Figures 1a-1b display the daily averaged sunspot number and Dst index, respectively. It can be observed that geomagnetic activities were relatively weak in 2009 corresponding to the beginning of the 24 solar cycle. Figure 1c shows the ten-days averaged trapped 206 keV electron fluxes measured in the SAA region (longitude = [320°, 330°], L=1.7). Hundreds of keV electron fluxes in the inner radiation belt generally experience quick increases during injections followed by slow decay during quiet times. However, the 206 keV energy channel was saturated before 2009 and thus showed only slight variations. From the middle of 2008 to the beginning of 2010, 206 keV electron fluxes mainly showed decreases with a weak increase in the middle of 2009 corresponding to a moderate geomagnetic storm (Dst around -50 nT) indicated by Figure 1b. After a

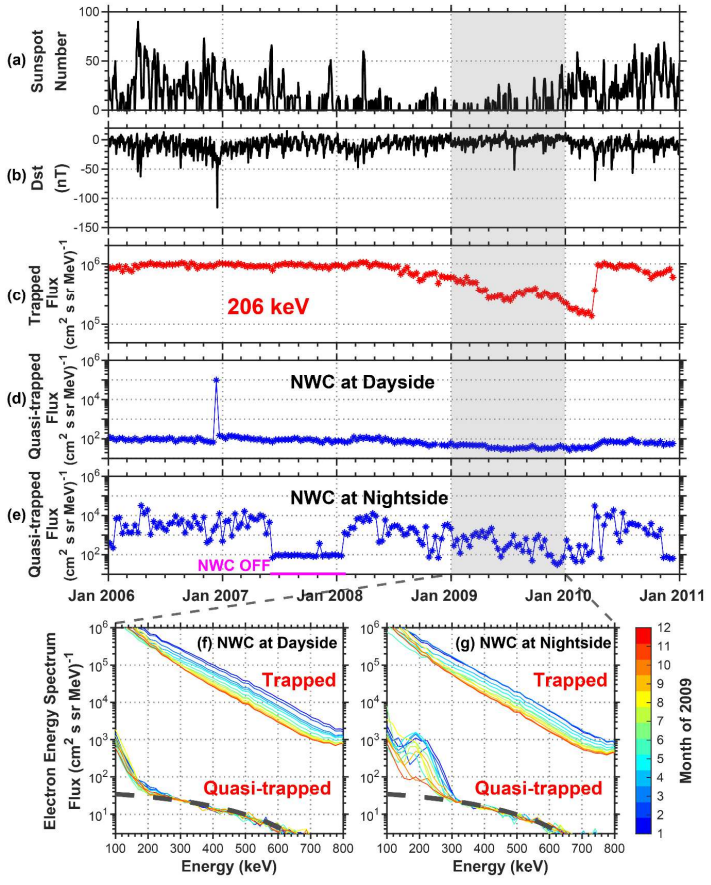

Figure 1. *(a) Sunspot numbers. (b) Dst index. (c) Ten-days averaged 206 keV trapped electron fluxes measured at longitude = [320°,330°] and L=1.7. (d and e) Ten-days averaged 206 keV quasi-trapped electron fluxes at longitude = [120°,130°] and L=1.7 when NWC was at dayside and nightside, respectively. The magenta line indicates when the NWC station operation was off. (f and g) The electron energy spectrum at L=1.7 during 2009 corresponding to NWC transmitter at dayside and nightside, respectively. The gray dash lines are the energy spectrum of CRAND-produced electrons.*

geomagnetic storm with Dst reaching -75 nT in the early 2010, 206 keV electron fluxes increased to the upper limit of IDP instrument again. It should be noted that the higher energy channels of IDP (e.g., 500 keV) were not saturated before 2009 and showed well correlations with solar cycles. Figure 1d and Figure 1e show ten-days averaged quasi-trapped electron fluxes (longitude = [120°, 130°], L=1.7, just east of NWC) when NWC station was at dayside (0500-1900 MLT) and nightside (1900-0500 MLT), respectively. Due to the lower total electron density in the ionosphere at the nightside, more VLF transmitter energies can leak into the magnetosphere and have stronger scattering effects on electrons in the inner radiation belt. The quasi-trapped 206 keV electron fluxes in Figure 1d stay around 10^2 (cm^2 s sr MeV)$^{-1}$ when NWC was at dayside, which is likely originated from the CRAND (Li et al., 2017), except a high flux data point at the end of 2006 corresponding to a strong geomagnetic storm during which electrons at higher L can penetrate into the low L driven by convection electric field. Different from NWC at dayside, quasi-trapped electron flux levels are 1-2 orders of magnitude higher when NWC is at nightside (Figure 1e). During June 2007 to January 2008, the NWC operation was off and the quasi-trapped electron fluxes in Figure 1d and Figure 1e are comparable, suggesting that CRAND possibly are the main source of quasi-trapped 206 keV electrons without VLF transmitter signals in the inner belt. To investigate the variations of electrons at other energies during 2009, we plot the energy spectrum evolutions of trapped and quasi-trapped electrons in Figures 1f-1g. The curve group with higher fluxes is the energy spectra of trapped electrons while the lower part is quasi-trapped electrons. The gray dash line is the energy spectrum of CRAND-produced electrons. When NWC station was at dayside (Figure 1f), it is evident that the DEMETER observations of >200keV quasi-trapped electrons fit well with the energy spectrum of CRAND-produced electrons, suggesting that these electrons are likely from CRAND. In Figure 1g, a striking bulge appears around 100-300 keV with a peak around 200 keV in the energy spectrum of quasi-trapped electrons. These electron fluxes show a similar decrease trend with the trapped electrons, indicating that these quasi-trapped electrons are scattered from trapped electrons by NWC transmitter signals.

In this study, a drift-diffusion-source model [8] is adopted to simulate the quasi-trapped electron distributions including the effect by CRAND and NWC transmitter signals. This model assumes that inner belt electrons are controlled by electron azimuthal drift, PA diffusion due to coulomb collisions with atmosphere and wave-particle interactions with NWC transmitter signals, and CRAND as a source. For a given L-shell and kinetic energy, the drift-diffusion-source model is governed by the following equation,

$$\frac{\partial J}{\partial t} + \omega_d \frac{\partial J}{\partial \phi} = -\frac{\partial}{\partial E}\left(J\frac{dE}{dt}\right) + S_e + \frac{1}{G_{0(\alpha_{eq})}\sin(2\alpha_{eq})}\frac{\partial}{\partial \alpha_{eq}}\left[G_0(\alpha_{eq})\sin(2\alpha_{eq})\langle D_{\alpha\alpha}\rangle\frac{\partial J}{\partial \alpha_{eq}}\right], \quad (1)$$

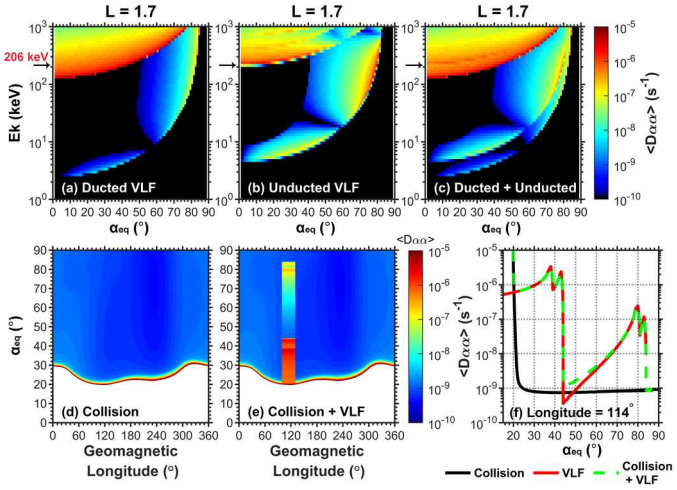

Figure 2. *The color-coded bounce-averaged quasi-linear pitch angle diffusion coefficient* $\langle \boldsymbol{D_{\alpha\alpha}} \rangle$ *as a function of equatorial pitch angle* $\boldsymbol{\alpha_{eq}}$ *and kinetic energy* $\boldsymbol{E_k}$ *from (a) ducted waves, (b) unducted waves, and (c) a combination of 75% ducted and 25% unducted VLF waves. The color-coded* $\langle \boldsymbol{D_{\alpha\alpha}} \rangle$ *of 206 keV electrons as a function of geomagnetic longitude and* $\boldsymbol{\alpha_{eq}}$ *from (d) collisions; (e) collisions and VLF waves. The vertical bar in (e) represents* $\langle \boldsymbol{D_{\alpha\alpha}} \rangle$ *induced by VLF waves in longitude range of [99°, 129°]. (f)* $\langle \boldsymbol{D_{\alpha\alpha}} \rangle$ *as a function of* $\boldsymbol{\alpha_{eq}}$ *at longitude=114°.*

where J is electron flux, ω_d is the bounced-averaged drift frequency, ϕ is the geomagnetic longitude, α_{eq} is the equatorial pitch angle (PA), $G_0(\alpha_{eq}) = \frac{v\tau_b}{2}$ and τ_b is the bonce period, v is the electron speed. S_e is the electron source rate from CRAND. The $\langle D_{\alpha\alpha} \rangle$ of electrons induced by NWC transmitter signals is calculated using the Full Diffusion Code (e.g. [3], [4]). The VLF waves are assumed to have a Gaussian frequency distribution, centered at the NWC transmit frequency (19.8 kHz) and the bandwidth is 100 Hz. The wave amplitude is set as 10 pT firstly and will be adjusted in the simulation. Figures 2a-2c show the color-coded $\langle D_{\alpha\alpha} \rangle$ as a function of electron equatorial PA α_{eq} and kinetic energy E_k from ducted waves, unducted waves, and a combination of 75% ducted and 25% unducted VLF waves, respectively [9]. These results suggest that the ducted VLF waves can efficiently scatter the 206 keV trapped electrons. Thus, we apply the $\langle D_{\alpha\alpha} \rangle$ of 206 keV electrons shown in Figure 2c into the simulation. Figures 2d-2e are the color-coded $\langle D_{\alpha\alpha} \rangle$ of 206 keV electrons as a function of geomagnetic longitude and $\langle D_{\alpha\alpha} \rangle$ from collisions and VLF waves, respectively, the blank part is BLC that calculated based on International Geomagnetic Reference Field (IGRF) model, corresponding to the equatorial PA of electrons which loss into atmosphere at 100 km altitude. Figure 2f shows the $\langle D_{\alpha\alpha} \rangle$ as a function of electron equatorial PA α_{eq} at longitude=114° as an example, the strong $\langle D_{\alpha\alpha} \rangle$ near the loss cone is from the collision and the $\langle D_{\alpha\alpha} \rangle$ between the loss cone and PA=44 ° is due to cyclotron resonance while the strong parts at higher PAs are from Landau resonance.

3. Simulation Results

We compare simulation results with observations from DEMETER in Figure 4. From top to bottom, the panels show simulation results with different VLF wave amplitude: 0 pT, 10 pT, 15 pT, 20 pT. The simulation result with 0 pT VLF wave amplitude represents the condition when NWC station is at dayside and no VLF transmitter signal leaks into the magnetosphere. The hollow triangles in left panels of Figure 4 represent the equatorial PAs of electrons measured by DEMETER at L=1.7 during each pass on 19 March 2009, which incorporate the actual detector looking directions and IGRF magnetic model (Tu et al., 2010; Xiang et al., 2019). The upward and downward triangle in Figure 4 indicate observations in the northern and southern hemispheres, respectively. The electron fluxes corresponding to the hollow triangles in the left column are plotted as a function of geomagnetic longitude and shown in the right column of Figure 4. The solid and

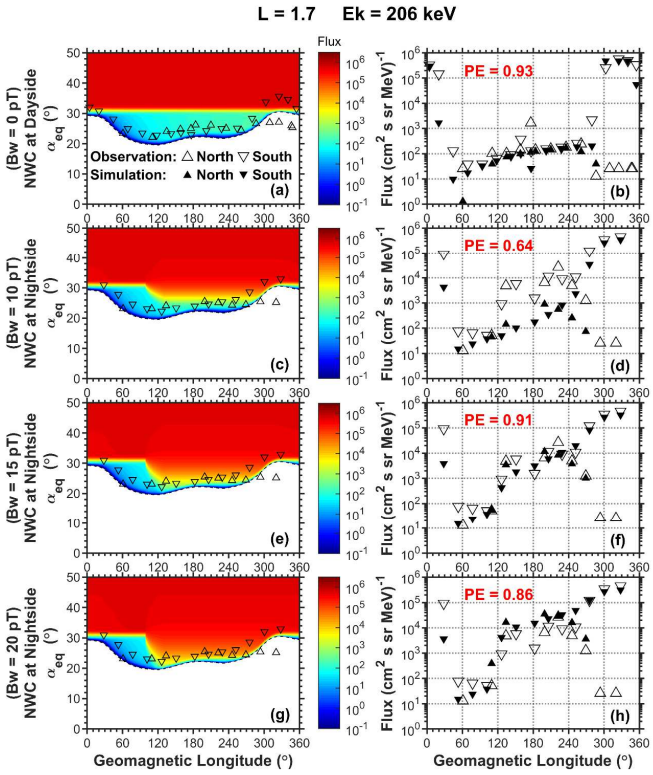

Figure 3. *(left column) Simulated electron fluxes distribution with different VLF wave amplitudes, from top to bottom is (a) 0 pT, (b) 10 pT, (c) 15 pT, and (d) 20 pT respectively. The hollow triangles represent the equatorial PAs of electrons measured by DEMETER at L=1.7 during each pass on 19 March 2009. (right column) Comparisons between the longitudinal distribution of simulated fluxes (solid triangle) that corresponding to the hollow triangles in the left panel and the observations (hollow triangle) from DEMETER. The upward and downward triangles indicate in the northern and southern hemispheres, respectively. PE is the goodness of fit between simulated results and DEMETER measurements.*

hollow triangles represent the simulation and observation results respectively. The dayside simulation results have good agreements with observations and the PE we get through equation (3) is 0.93, suggesting that CRAND is the main source of quasi-trapped electrons at L=1.7 when NWC is at dayside. We add $\langle D_{\alpha\alpha} \rangle$ from VLF waves to simulate the situation that NWC transmitter is at nightside. Firstly, we set the VLF amplitude to 10 pT (Figure 4c-4d), the comparison between simulation results and the observations indicates that the scattering effect of VLF wave is not enough (PE=0.64). The simulations agree well with observations at around 15 pT (PE=0.91) (Figure 4e-4h). The results suggest that the scattering effect of VLF is the dominant source of the quasi-trapped electrons when NWC is at nightside during the quiet period. The $\langle D_{\alpha\alpha} \rangle$ from VLF waves should be as strong as ~10^{-6}-10^{-5} s^{-1} to scatter enough trapped electrons into the DLC.

4. Discussions and Conclusions

In this study, we simulate longitudinal distributions of 206 keV quasi-trapped electrons at L=1.7 using a drift-diffusion-source model and compare the results with DEMETER observations. The good agreement between simulations and observations suggest that the ~200-700 keV quasi-trapped electrons at L=1.7 are mainly from the CRAND without influences from NWC. In contrast, ~200 keV quasi-trapped electrons are mainly induced by pitch angle diffusions when NWC transmitter operates at nightside.

Based on the calculation results of pitch angle diffusion coefficients in Figure 2a-2b, we found that the scattering effects from ducted waves are much stronger than unducted waves. Using PROBA-V satellite observations, Cunningham et al., [10] found that enhanced 500-800 keV electron fluxes at L ≈ 1.54, suggesting that the ducted interactions at L<1.55 and unducted interactions at L>1.65. In this study, we assume 25% unducted waves and 75% ducted waves in the simulation following previous studies [9]. The exact wave normal angle distribution of VLF transmitter signals in the magnetosphere is needed to accurately quantify the scattering effect on electrons.

5. Acknowledgements

This work was supported by NSFC grant 41904143 and 42174190.

6. References

[1] Selesnick, R. S., Blake, J. B., & Mewaldt, R. A. (2003). Atmospheric losses of radiation belt electrons. Journal of Geophysical Research, 108(A12), 1468, doi:10.1029/2003JA010160

[2] Xiang, Z., Li, X., Selesnick, R., Temerin, M. A., Ni, B., Zhao, H., et al. (2019). Modeling the quasi - trapped electron fluxes from cosmic ray albedo neutron decay (CRAND). Geophysical Research Letters, 46, 1919 - 1928. https://doi.org/10.1029/2018GL081730

[3] Ni, B., Thorne, R. M., Shprits, Y. Y., & Bortnik, J. (2008). Resonant scattering of plasma sheet electrons by whistler-mode chorus: Contribution to diffuse auroral precipitation. Geophysical Research Letters, 35, L11106. https://doi.org/10.1029/2008GL034032

[4] Ni, B., Cao, X., Zou, Z., Zhou, C., Gu, X., Bortnik, J., et al. (2015). Resonant scattering of outer zone relativistic electrons by multiband EMIC waves and resultant electron loss time scales. Journal of Geophysical Research: Space Physics, 120, 7357–7373. https://doi.org/10.1002/2015JA021466.

[5] Li, X., Selesnick, R., Schiller, Q., Zhang, K., Zhao, H., Baker, D. N. et al. (2017). Measurement of electrons from albedo neutron decay and neutron density in near-Earth space. Nature, 552, 382–385. https://doi.org/10.1038/nature24642

[6] Tu, W., Selesnick, R., Li, X., & Looper, M. (2010). Quantification of the precipitation loss of radiation belt electrons observed by SAMPEX. Journal of Geophysical Research, 115, A07210. https://doi.org/10.1029/2009JA014949

[7] Selesnick, R. S., Albert, J. M., & Starks, M. J. (2013). Influence of a ground-based VLF radio transmitter on the inner electron radiation belt. Journal of Geophysical Research: Space Physics, 118, 628–635. https://doi.org/10.1002/jgra.50095

[8] Xiang, Z., Li, X., Temerin, M. A., Ni, B., Zhao, H., Zhang, K., et al. (2020). On energetic electron dynamics during geomagnetic quiet times in Earth's inner radiation belt due to atmospheric collisional loss and cosmic ray albedo neutron decay (CRAND) as a source. *Journal of Geophysical Research: Space Physics*, 125, e2019JA027678. https://doi.org/10.1029/2019JA027678

[9] Ma, Q., Mourenas, D., Li, W., Artemyev, A., & Thorne, R. M. (2017). VLF waves from ground-based transmitters observed by the Van Allen Probes: Statistical model and effects on plasmaspheric electrons. Geophysical Research Letters, 44, 6483–6491. https://doi.org/10.1002/2017GL073885

[10] Cunningham, G. S., Botek, E., Pierrard, V., Cully, C., & Ripoll, J.-F. (2020). Observation of high-energy electrons precipitated by NWC transmitter from PROBA-V low-Earth orbit satellite. Geophysical Research Letters, 47, e2020GL089077. https://doi.org/10.1029/2020GL089077